
1. INTRODUCTION

Acoustic vector sensors are devices used to measure both the particle motion and the sound pressure, while hydrophones are omni directional and measure only the sound pressure. Therefore, directional information of the acoustic field may be extracted with a vector sensor. Particle velocity measurements along each of the three axes (spatial derivative of the pressure) can be determined using pairs of hydrophones (whose distance should be less than four times the minimum wavelength¹) for each axis or by using tri-axial accelerometers. The vector sensor (VS) based on a combination of an hydrophone and an accelerometer assembled in a single encasing is, currently, the most common device². The advantage of a vector sensor compared with an hydrophone is the quantity of information obtained in a single point of space.

Since the 90's, the spatial filtering capabilities of vector sensors are being investigated and theoretical works appeared in the scientific community, first in electromagnetic propagation³ and then in underwater acoustic signal processing^{4,5}. Most research involving vector sensors is related to direction of arrival (DOA) estimation, since the combination of several vector sensors in a vector sensor array (VSA) allows to estimate both azimuth and elevation angles, eliminating the well know left/right ambiguity that exists with linear hydrophone arrays^{6,7}. Taking advantage of its directionality and its high performance in DOA estimation, the use of VS and VSA appear in other underwater applications, using simulated or experimental data such as narrowband detection of acoustic sources^{8,9}, source tracking¹⁰, underwater communications^{11,12} and geo-acoustic inversion^{13,14}. Santos *et al.*¹⁴ demonstrated with experimental data acquired in the frequency band 8-14 kHz that sediment parameters can be estimated with higher resolution using an array of four VS than an array with the same number of hydrophones. Recently, it was demonstrated that the combination of particle velocity with pressure or with particle velocity gradient is useful for multi-path discrimination, where the bottom-reflected paths are improved, important for example in geophysical research applications.¹⁵

Nowadays, ocean geophysical exploration systems are usually formed as a series of long cables of horizontal hydrophones (known as streamers) towed by a single ship. Depending on seismic surveys, the use of a single or multiple sources with single or multiples streamers behind the sources are considered¹⁶. The operation of such complex systems is costly and imposes several constraints in terms of minimum water depth and ship maneuvering for reliable and safe operation, particularly in coastal areas. The European project WiMUST (Widely scalable Mobile Underwater Sonar Technology) aims to simplify and to improve the efficacy of actual geo-acoustic surveys through the use of autonomous underwater vehicles (AUVs) for towing short streamers in a distributed configuration.

In the framework of the WiMUST project, a Dual Accelerometer Vector Sensor (DAVS) was developed in order to complement the streamers' data, allowing for the reduction of their size and facilitating the operation of the WiMUST distributed configuration¹⁷. The use of a dual accelerometer configuration with a single hydrophone, known as the DAVS system, was based on a previous study¹⁵, which showed that a combination of the particle velocity with pressure or with the particle velocity gradient has the ability to cancel or significantly attenuate the direct and the surface-reflected paths, improving bottom-reflected paths useful for seismic imaging. Additionally, the compact configuration of the DAVS allows for easy mounting and operation on AUVs.

The objective of this work is to present experimental results of functionality tests which were performed with the DAVS system. The first test took place in an anechoic tank of the naval base of "Arsenal do Alfeite", Lisbon (Portugal), where the objective was to measure the directivity and the sensitivity of each sensor component on the DAVS. The device was suspended in a carriage system in front of a source, which emitted tone signals between 1 and 4 kHz. The radiation diagrams for the hydrophone and for each particle velocity components were obtained and are in line with the theory. . The second test took place in the *Oceanarium* marina shallow pond, Lisbon (Portugal), where the main objective was to test the response of DAVS directivity and to present experimental results on the estimation of azimuthal directions when the DAVS was in motion and attached to an AUV. Signals in the 1-2 kHz band were emitted by a Lubell 916C

source deployed at 1.5 m depth and acquired by the DAVS mounted on a MEDUSA class AUV, developed by ISR/IST, Lisbon (Portugal), which was following a pre-programed path with a 0.26 m/s nominal speed¹⁸. The azimuth estimates are coherent with the MEDUSA trajectories even in curved paths where the thruster's noise increases. Moreover, preliminary results for bottom characterization of the *Oceanarium* shallow pond obtained from combinations of particle velocity and particle velocity gradient from DAVS outputs will be also presented.

The paper is organized as follows. Section 2 presents the Dual Accelerometer Vector Sensor prototype and gives theoretical foundations for the dual accelerometer configuration. Section 3 is dedicated to the experimental results where the data acquired in the calibration experiment and in the field test are analyzed. Section 4 draws some conclusions.

2. DUAL ACCELEROMETER VECTOR SENSOR PROTOTYPE

The dual accelerometer configuration of the DAVS was based on the conclusions obtained from a previous work¹⁵. It was seen that a combination of particle velocity with the particle velocity gradient has advantages in direct and surface-reflected paths attenuation in contrast with the improvements verified in bottom-reflected paths. Additionally, the DAVS system should be compact to be easily mounted on an AUV in order to facilitate the WiMUST distributed configuration.

Figure 1 (a) shows a photo of the DAVS system where it can be seen two main parts: the acoustic active part (black nose) and the container (white tube). The acoustic active part is constituted by two tri-axial accelerometers (gray blocks) and by an in-house build hydrophone (yellow cylindrical component) between them, as presented in Fig. 1 (b). The orientation of the accelerometers components relatively to the Cartesian system is also shown on the inserted, where the x -axis is pointing to the front nose, the y -axis is pointing to us and the z -axis is pointing from the #49 to the #50th accelerometer. The DAVS system overview, the characteristics of the sensors, the electronic part, the connections, the acquisition system and the power supply are described in detail in¹⁷.

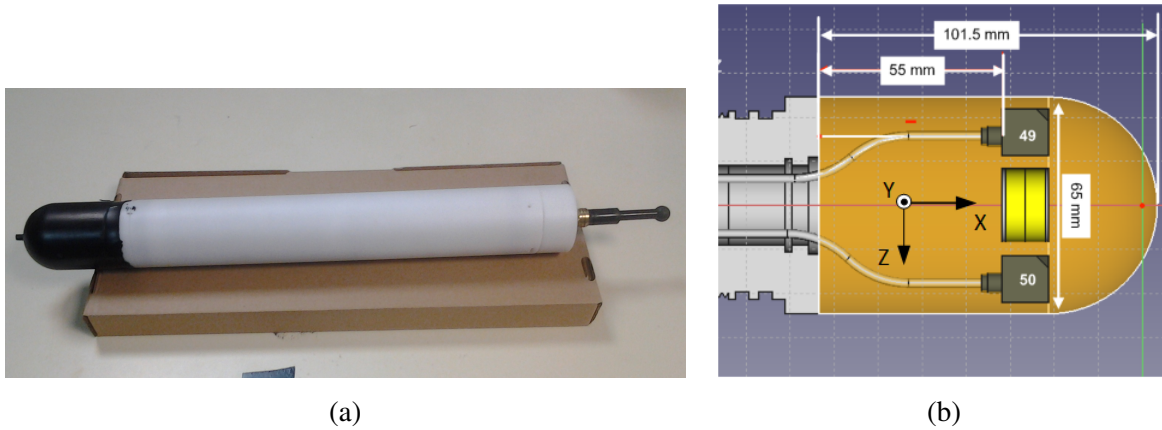


Figura 1: A photo of the Dual Accelerometer Vector Sensor (DAVS) system (a) and the internal view of the acoustic part (black nose), where it is seen the two accelerometers (gray blocks, numbered as #49 and #50) and the hydrophone (yellow cylindrical) and their position relatively to the Cartesian coordinate system (b). The x -axis is pointing to the front nose, the y -axis is pointing to us and the z -axis is pointing from the #49 to the #50th accelerometer.

A. DAVS - A DUAL ACCELEROMETER CONFIGURATION

The theoretical foundation which is in the base of the dual accelerometer configuration of the DAVS system was presented in¹⁵. The combination of the particle velocity with the pressure or with the particle velocity gradient allows to attenuate the direct and the surface reflections paths of the signal (undesired for bottom characterization such as in seismic geo-acoustic exploration) since they may interfere with bottom information. So, the use of two particle velocity sensors with an hydrophone between them, seems to be an usefull solution for this purpose¹⁵.

The pressure equivalent particle velocity, i.e., the particle velocity in pressure units can be obtained from acceleration, at a given frequency ω , by:

$$\hat{V}_i(\omega) = \frac{\rho c}{j\omega} A_i(\omega) = \frac{\rho}{jk} A_i(\omega), \quad (1)$$

where $i = x, y$ or z -axis, $k = \frac{\omega}{c}$ is the wavenumber, c is the water sound speed, ρ is the water density and ρc is the scaling factor according to the definition of acoustic impedance. For simplification, in the following only one axis (in this case the vertical axis) will be considered, but the formulation can be generically performed for all axes. The particle velocity can be combined with the particle velocity difference or particle velocity gradient, where two particle velocity sensors (V_{z1} and V_{z2}) are at close locations (D separation), by:¹⁵

$$\tilde{V}(\omega) = \frac{V_{z1}(\omega) + V_{z2}(\omega)}{2} + \frac{1}{jk} \frac{V_{z1}(\omega) - V_{z2}(\omega)}{D}, \quad (2)$$

or combined with the pressure ($P(\omega)$), using the hydrophone and the accelerometers information from the DAVS outputs, as:

$$\tilde{P}(\omega) = P(\omega) + \frac{V_{z1}(\omega) + V_{z2}(\omega)}{2}. \quad (3)$$

The directivity patterns or radiation diagrams characteristics of sensors or sensor arrangements can be obtained normalizing the amplitude as $|B(\omega, \phi)|/\max(|B(\omega, \phi)|)$, where $B(\omega, \phi)$ is the beam pattern for each combination of sensors. In our case, Fig. 2 compares the normalized amplitude directivity pattern from the pressure only (blue line), the particle velocity component (1) (green line), the combination of particle velocity with the particle velocity difference (2) (red line) and the combination of pressure with the particle velocity component (3) (black line). This directivity pattern was obtained considering all the sensors aligned with the vertical axis, where the maximum response is obtained for 90° .

It can be seen that the pressure presents the typical omnidirectional pattern and the particle velocity shows a typical “figure of eight” shaped directivity pattern, whereas the combination of particle velocity and particle velocity gradient or the combination of pressure and particle velocity show a “cardioid” shaped directivity, having the former combination a narrower main lobe than the latter. Considering an application for bottom characterization, on one hand, a combination of particle velocity sensors aligned with the vertical axis allows to cancel (or significantly attenuate) the direct path and surface-reflected paths, usually considered as a nuisance. On the other hand, the particle velocity sensors in a horizontal arrangement would cancel the latter arrivals, and when combined with pressure or particle velocity gradient can be used to cancel arrivals from noise sources in opposite directions of the active source.

3. DAVS EXPERIMENTAL RESULTS

This section is dedicated to the results of the functionality tests undertaken with the DAVS system. The first test was a calibration test that took place in an anechoic tank in Lisbon (Portugal), where the objective was to measure the sensitivity of each sensor and to measure the directivity of each accelerometer component on the DAVS. The second test was a field test in the *Oceanarium* marina shallow pond, Lisbon (Portugal),

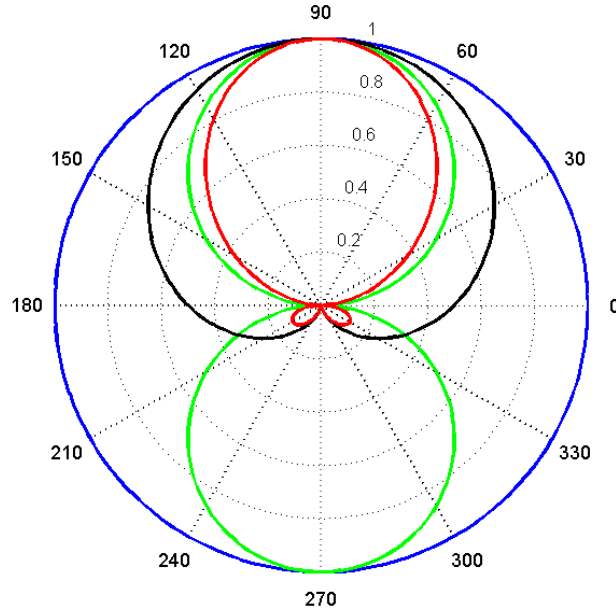


Figura 2: Normalized amplitude directivity patterns for an arrangement of sensors placed along the vertical axis (90°) considering: pressure only (blue line), particle velocity component (green line), combination of particle velocity and particle velocity difference (red line) and combination of pressure and particle velocity component (black line).

where the objective was to test the response of DAVS directivity and to present experimental results on the estimation of azimuthal directions when the DAVS is in motion mounted on an AUV.

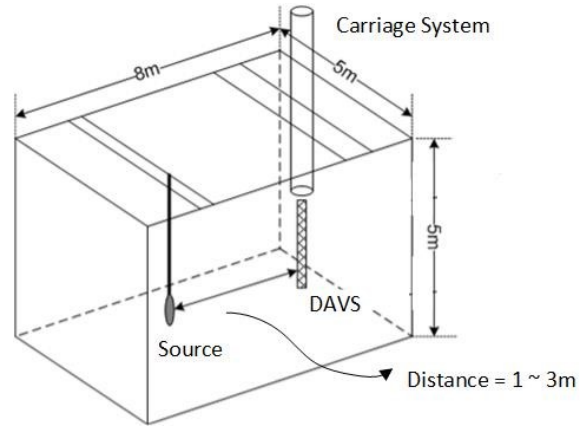
A. CALIBRATION TEST

The calibration test took place in the anechoic tank of naval base of “Arsenal do Alfeite”, Lisbon, at the beginning of September 2016, Fig. 3. The tank is covered on all sides including the surface by anechoic panels and it has dimensions of 8 m length, 5 m wide and 5 m depth, as shown in Fig. 3 (a) and (b), respectively. The source was positioned in front of the device at ranges between 1 and 3 m and the DAVS was suspended in a rotating carriage system, both at 2.5 m depth. The source emitted 20 cycles of tone signals at 1, 2, 3 and 4 kHz. The DAVS accelerometer components’ orientation relatively to the source is shown in Fig. 4, where it can be seen that the x component is pointing to the bottom and the source signal is impinging first in accelerometer #50 on z -axis (the z and y components define the rotation plane) and then rotates 360° . Since the suspension of the DAVS in the carriage system was only possible in this configuration, the x component directivity was not measured. The procedure scheme of the calibration test is described in detail in¹⁷ as well as the hydrophone and the accelerometers sensitivity.

Figure 5 presents the normalized radiation diagrams in dB scale for the hydrophone and particle velocity components at two different frequencies, 1 kHz (left) and 2 kHz (right), and when the source and receiver range was 2 m. The results for the hydrophone (green dots) and x particle velocity component (blue dots for accelerometer #49 and red dots for #50) are presented in Fig. 5 (a) and (b), while (c) and (d) present the normalized radiation diagram for y particle velocity components and (e) and (f) for z particle velocity components, considering blue and red dots for accelerometer #49 and #50, respectively, and superimposed with green dots for the theoretical radiation diagram. The green dots in plots (a) and (b) give the typical



(a)



(b)

Figura 3: A photo of the anechoic tank showing the panels at the surface (a) and the tank dimensions where it is seen the position of the source and the rotating carriage system that suspended the DAVS (b).

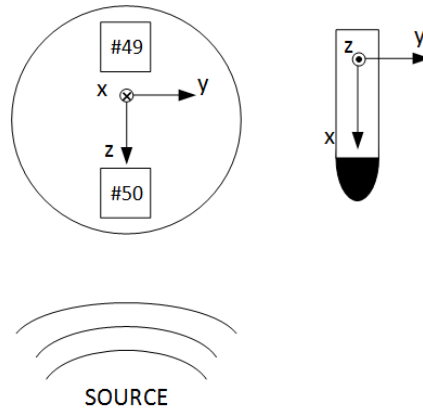


Figura 4: The orientation of the DAVS components at start position relative to the source in the calibration test with the DAVS coordinate system, where the x -component is pointing to the bottom and the y and z -components were in the horizontal plane (rotation plane).

omnidirectional response of the hydrophone. Although the scheme of the calibration test was not able to measure the x component directivity, these plots present also the normalized radiation diagram of this component for #49 and #50 accelerometer (blue and red dots, respectively), showing that this component is not sensitive to the incident acoustic wave in the y - z plane.

The source signal impinges the z components at 0° and 180° , being the y component maxima obtained for -90° and 90° , as shown in Fig. 5 (c) to (f). The results at all angles follow almost the typical theoretical “figure of eight” radiation diagram of the particle velocity components. However, there is some asymmetry in those radiation diagrams due to possible effects from external sources of noise. Moreover, some differences in the amplitudes between the two accelerometers responses appear due to possible shadow effects (mainly at 0° caused by accelerometer #50 over #49 at 1 kHz), nevertheless these responses are improved and are mostly equal between accelerometers for the frequency of 2 kHz (left side of Fig. 5). The radiation diagrams for individual accelerometers components were obtained and they are in line with theory.

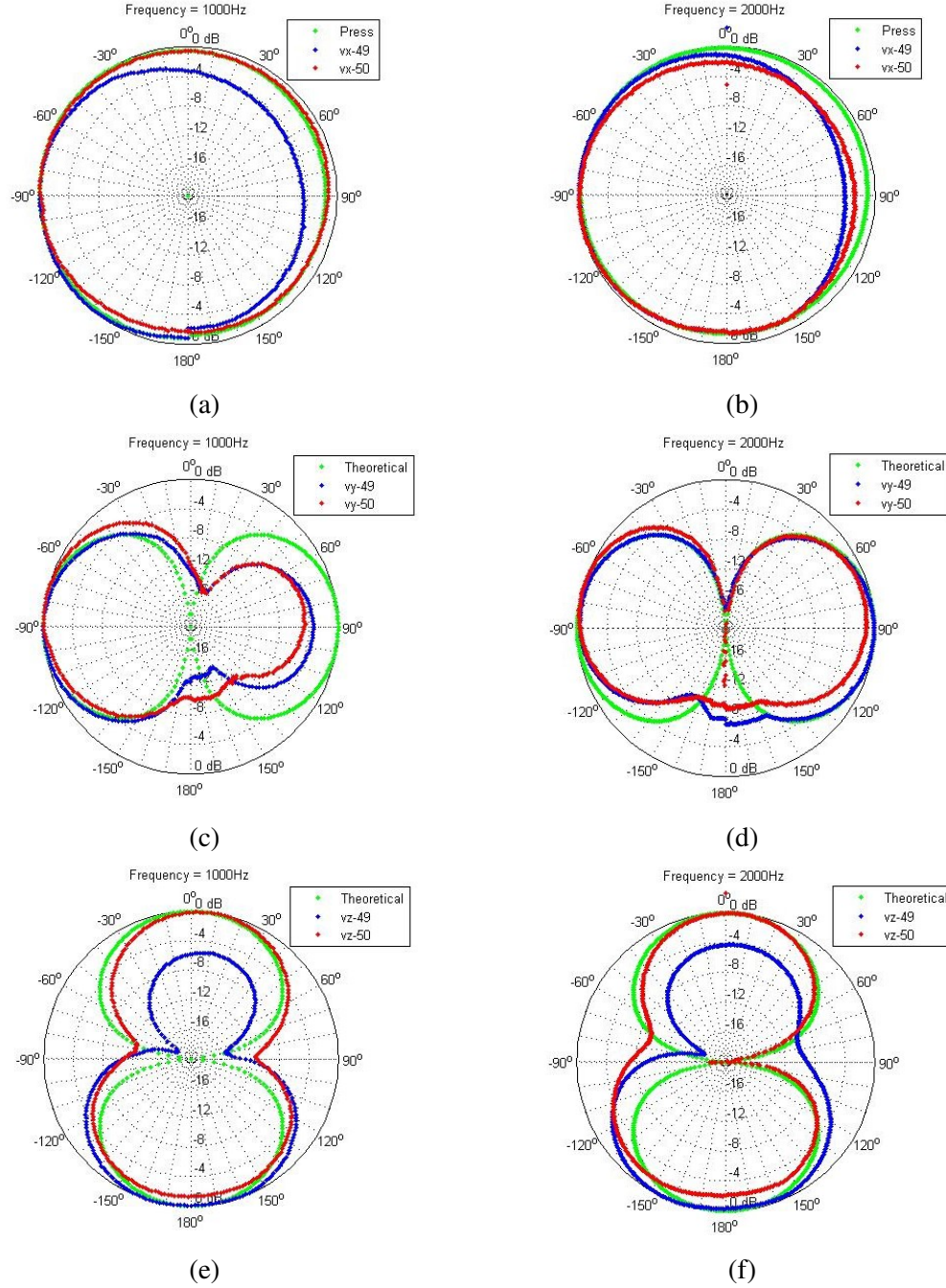


Figura 5: Normalized radiation diagrams for the hydrophone and each particle velocity components for two different frequencies, 1 kHz and 2 kHz, left and right plots respectively. The hydrophone (green dots) and particle velocity x -components responses (#49 and #50 blue and red dots, respectively) (a) and (b), theoretical (green dots) and particle velocity components' responses (#49 and #50 blue and red dots, respectively) for y -components (c) and (d), and z -components (e) and (f).

B. LISBON FIELD TEST

The experiment field test realized with the DAVS prototype took place at the *Oceanarium* marina, “Parque das Nações”, Lisbon, in September, 2016, where the objective was to evaluated its azimuthal direction

estimation capabilities when the DAVS was in motion attached on an AUV. Figure 6 shows a satellite view of the marina, where the yellow box delimits the area used for the experiment and the red dot shows the acoustic source (Lubell 916C) location. The Lubell 916C source was deployed at 1.5 m in a water depth of approximately 3 m and emitted a sequence of 3 minutes of linear frequency modulated (LFM) up sweeps signal in the 1-2kHz frequency band and 3 minutes of gated signals of a single 2 kHz tone in a repeated sequence: 10 ms signal duration followed by 397ms of silence.



Figura 6: *The location of the experiment test delimited by the yellow line, inside of the Oceanarium marina, “Parque das Nações”, Lisbon, where the red dot shows the location of the Lubell 916C source .*

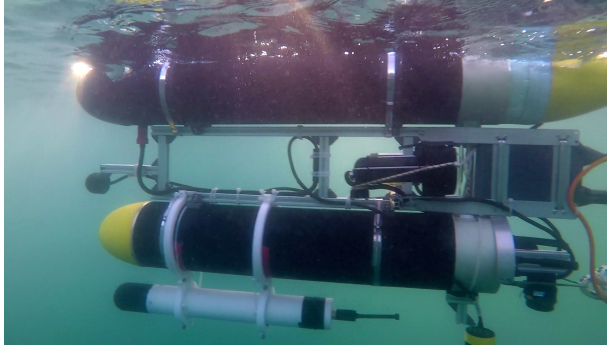
During the Lisbon experiment, the DAVS was mounted on the MEDUSA class AUV¹⁸, provided by ISR/IST, University of Lisbon. A photo of the MEDUDA during the experiment with the DAVS mounted below at approximately 0.5 m depth is presented in Fig. 7 (a). The AUV follows a pre-programed trajectory (so-called “Butterfly” trajectory) at 0.26 m/s nominal speed. The top view of the generic AUV trajectory relatively to the source position at the origin of the Cartesian coordinate system (marked by (*)) is given by the blue line in Fig. 7 (b). The AUV trajectory starts at position $(-38; -45)$ m, marked by (o) and ends at $(34; -17)$ m, marked by (□). Next, the AUV follows the trajectory given by the blue line with the time evolution from “Track 1” to “Track 5”. The tracks that will be analyzed in more detail in this work are Tracks 4 and 5, marked by a dash circle in Fig. 7 (b).

In this experiment, the x and y DAVS components were parallel to the X - Y experiment plane (Top view of AUV trajectory), as drawn in Fig. 8. The positive z -axis points to the surface and the positive x -axis points to the sailing direction. The DAVS was positioned on the AUV such that the two accelerometers and the hydrophone were aligned with the vertical z -axis, being the #50 the shallowest accelerometer, as shown in Fig. 8.

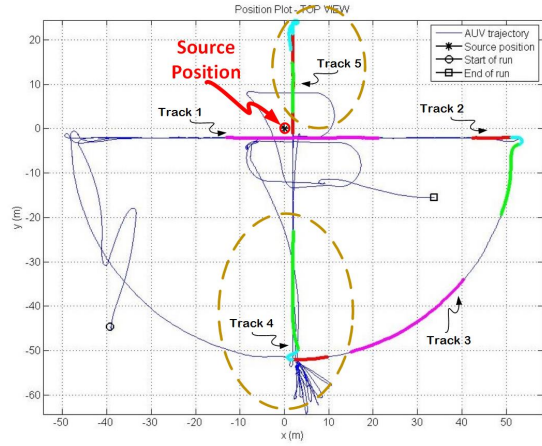
The azimuth angle estimation, for the several tracks presented above, was evaluated using the Intensity-based estimator described in¹⁹. As a first processing step, the acceleration components (three for each accelerometer) were converted to particle velocity components first by using their Fourier Transform to the frequency domain, then by using (1), and then back to time domain. The pressure and all particle velocity components were filtered using a band-pass filter of 1-2 kHz and a matched-filtered with the emitted signal. Then, the pressure $p(t)$ is cross-correlated at lag 0 with $v_x(t)$ and with the $v_y(t)$ particle velocity components, and an estimation of the azimuthal direction of the source signal, Θ_S at large SNR is given by:

$$\hat{\Theta}_S = \arctan 2 \frac{\langle v_y(t)p(t) \rangle}{\langle v_x(t)p(t) \rangle}, \quad (4)$$

where $\langle \rangle$ stands for time averaging.



(a)



(b)

Figura 7: A photo of the MEDUSA class AUV provided by ISR/IST used during the Lisbon experiment with the DAVS mounted below the AUV (a) and the top view of AUV “Butterfly” trajectory relatively to the source position at the origin of coordinate system (marked by (*)) (b). The AUV run starts at location marked (o) and ends at location marked (□). The run from Track 1 to Track 5 shows the time evolution.

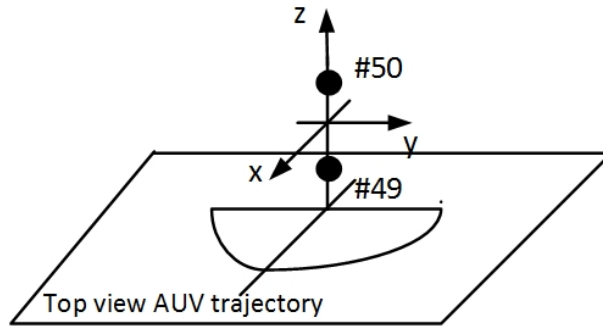


Figura 8: Drawing of the experiment X-Y plane (Top view of AUV trajectory) parallel to the DAVS x-y plane and the accelerometers are aligned with the vertical z axis, being the #50th the shallowest one.

i. Track 4

The received signal on Track 4 was a sequence of LFM signals in the 1-2 kHz band with 150 s time duration, as shown in the spectrogram received on the pressure sensor, Fig. 9 (a). The spectrogram shows that the thrusters’ frequency noise of the AUV appears for frequencies below 500 Hz, out of the active signal frequency band. However, before 40 s the noise level increases, mainly in the band of the emitted signal timely corresponding to the curved path illustrated by the cyan line in Fig. 9 (b). Figure 9 (b) shows the top view of the AUV’s trajectory, corresponding to three different paths given by red, cyan and green lines, where the DAVS accelerometers’ orientation relatively to the source position (origin of the coordinate system) is shown as an insert.

The results of the azimuth estimation of Track 4, 150 s of LFMs, is presented in Fig. 9 (c). The blue and red dots are the results of the estimation, considering the combination of the pressure with the particle velocity components given by (4) using #49 and #50 outputs, respectively. These results agree with the green dots, which were obtained from the Yaw AUV’s data and the positional information of the AUV’s

GPS data. The sequence of paths along the trajectory can be observed with an increase of 120° after 30 s, related with the sharp turn given by the cyan line, and then an adjustment to 0° corresponding to the green straight line, when the AUV approaches the source. From these results, it can be concluded that the azimuth estimates are in line with the considered true azimuth (given by the combination of the Yaw data and GPS data) and the thrusters' noise doesn't influence the azimuth estimations, even in the curved path where the noise level increases and superimposes on the signal frequency band.

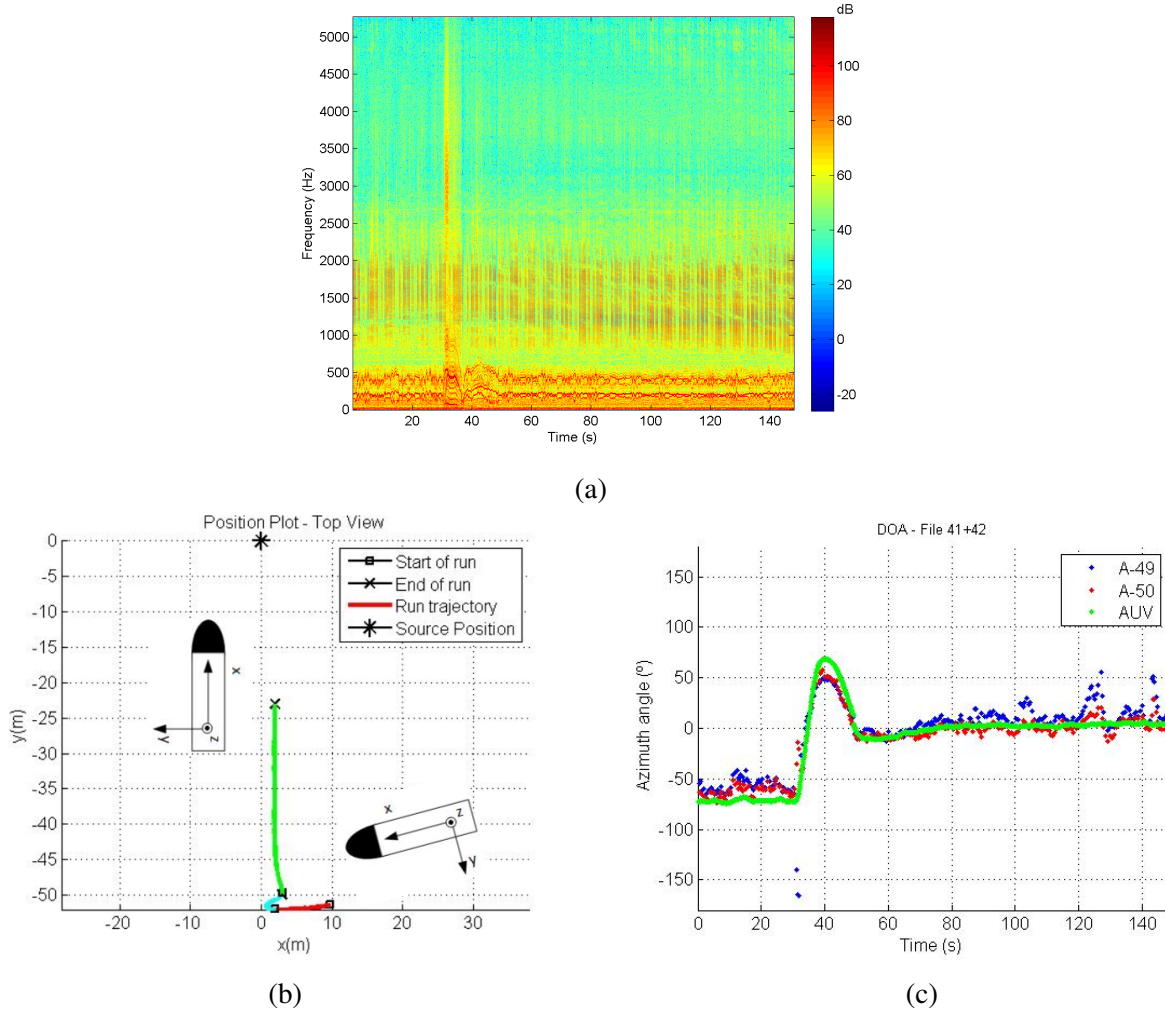


Figura 9: Track 4 - spectrogram of the received signal on the pressure sensor of DAVS (a), top view of the trajectory relative to the source position located at the origin of the Cartesian coordinate system, with the DAVS tri-axial system insert (b) and the estimation of the azimuth angle between the source and the AUV obtained using (4) for both accelerometers (blue dots for #49 and red dots for #50) combined with the heading angle from the Yaw AUV's data and the positional information of the AUV's GPS (green dots) (c).

ii. Track 5

In Track 5, the emitted signal was a 130 s long sequence of gated 2 kHz tonal signals and a 40 s long series of LFM up sweeps in the 1-2 kHz band, as shown in the spectrogram received on the pressure sensor,

Fig. 10 (a). It can also be seen that the signal from the thrusters' noise is below 500 Hz. Between 80 s and 100 s, the noise level increases, mainly in the band of the emitted signal, corresponding to the curved path illustrated by the cyan line in Fig. 10 (b), where the AUV performs a rotation of almost 300° in its trajectory. The DAVS accelerometers' orientation relative to the source position (origin of the coordinate system) is also inserted in the plot. This is a more complex trajectory, as seen in Fig. 10 (b), since the DAVS is first moving away from the source (green line) then performs a sharp turn (cyan line) with a rotation nearly 300° and at the end it is approaching the source (red line) superimposed in the initial run.

The results of the azimuth estimation for time duration of Track 5 are presented in Fig. 10 (c). The blue and red dots are the results of the estimation, considering the combination of the pressure with the particle velocity components given by (4) using #49 and #50 outputs, respectively. Although the DAVS has difficulties in the azimuth estimation, the results compare with the green dots assumed as the true azimuth (obtained from combination of the Yaw AUV's data and the position information of the AUV's GPS data), particularly at the end of the trajectory. The azimuth estimation errors seen until time 80 s are due to the fact that the source signal is impinging on the DAVS from the rear, when the white tube of Fig. 1 (a) shadows the acoustic sensor part (black nose). However, when the acoustic sensing part starts to be in line of sight with the source (after 80 s), the azimuth results follow the assumed true azimuth (green dots).

C. BOTTOM CHARACTERIZATION

As explained in section 2, the main objective of the dual accelerometer configuration of DAVS system is to improve the bottom characterization, where the combination of particle velocity with the particle velocity gradient allows to filter out undesirable direct and surface-reflected paths, improving the bottom-reflected paths. A pre-processing of bottom arrivals for bottom characterization is presented below considering part of Track 4, the straight green line of Fig. 9 (b).

The bottom characteristics of the *Oceanarium* marina is unknown but expected to be covered by a thin mud layer over a hard rock bottom. Comparison of the arrivals patterns obtained for the pressure only and for the combination of particle velocity and particle velocity gradient using (2) are shown in Fig. 11 (a) and (b), respectively. The advantage of the combination of particle velocity and particle velocity gradient over the pressure only can be seen of this figure as follows: 1) when the pressure only is used the high amplitude path refers to the direct path and the others paths are mostly attenuated, and 2) the combination of the particle velocity given by (2) in Fig. 11 (b), shows that the direct path is highly attenuated in contrast with the high amplitude obtained for the bottom reflection paths, mostly useful for bottom characterization. The bottom characterization using vector sensor information is ongoing work.

4. CONCLUSION

The objective of this work was to present experimental data of a recently developed prototype with a dual accelerometer's configuration, named as DAVS, from two functionality tests: a calibration test performed in an anechoic tank and a field test where the DAVS was mounted on an AUV.

The calibration test showed good results on directivity for the individual accelerometers components, where the horizontal components are in line with the theoretical "figure of eight" shaped directivity pattern. The sensitivity of the device for frequencies at 1 and 2 kHz was also measured and was 24 ± 1 mV/m/s² for the accelerometers components and -196 ± 2 dB re V/ μ Pa for the hydrophone.

The evaluation of the DAVS directivity in motion was achieved in the field test. The experiment results on the estimation of azimuthal directions for the different AUV's tracks showed good agreement and are inline with those obtained combining the heading angle with the position information of the AUV, considered as the true azimuth. It can be concluded that the thruster's noise does not influence neither disturbs the stability of the estimation results when DAVS is in motion, even in curved paths; the occurrence of some

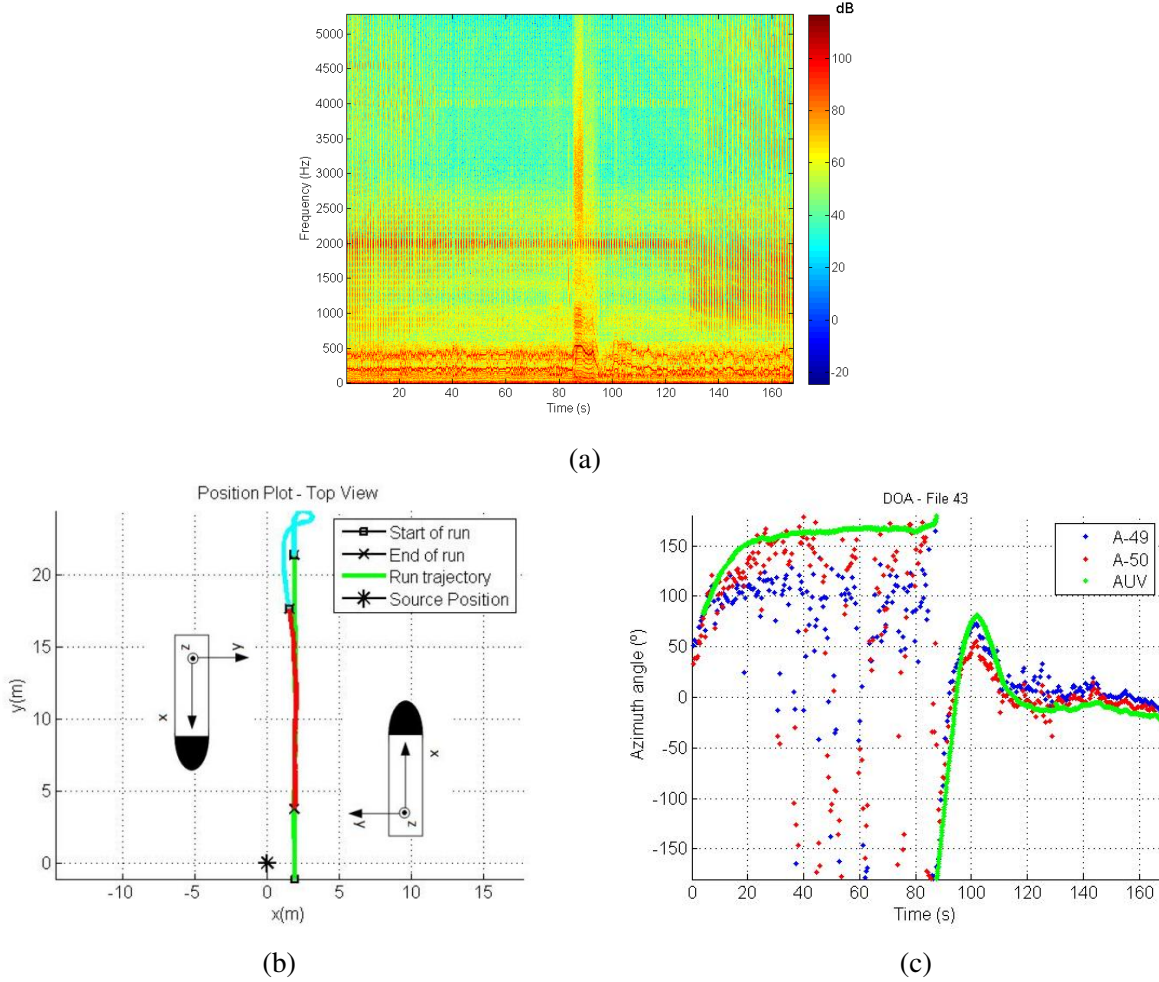


Figura 10: Track 5 - spectrogram of the received signal on the pressure sensor of DAVS (a), top view of the trajectory relative to the source position located at the origin of the Cartesian coordinate system, with the DAVS tri-axial system insert (b) and the estimation of the azimuth angle between the source and the AUV obtained using (4) for both accelerometers (blue dots for #49 and red dots for #50) combined with the heading angle from the Yaw AUV's data and the positional information of the AUV's GPS (green dots) (c).

variability on the results, in certain periods of time, appears when the signals are reaching from the rear of the DAVS; and the recorder housing (white tube) of the DAVS shadows the acoustic part (black nose). The tests indicate that, in general, the spatial directivity of the DAVS prototype is as expected.

Preliminary results for bottom characterization were also presented, showing the advantages of using the combination of particle velocity with particle velocity gradient when compared with the pressure only. This combination is useful for the direct and surface-reflected path attenuation in contrast with the improvements verified on bottom-reflected paths from the received waveforms. The effectiveness of the DAVS system and the use of particle velocity information for bottom characterization are the subject of ongoing research work.

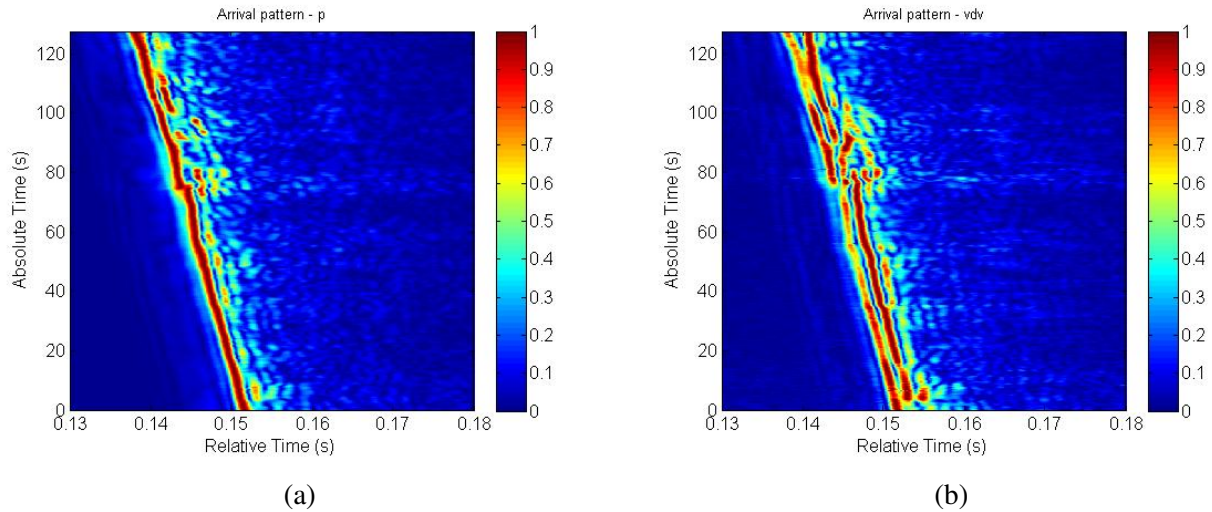


Figura 11: Arrival patterns in the time interval of the straight line (green line) of track 4, Fig. 9 (b), considering the pressure only (a) and the combination of particle velocity with the particle velocity gradient (b) given by (2).

ACKNOWLEDGMENTS

The authors would like to thank ISR/IST, University of Lisbon, for the use of MEDUSA class AUV and providing assistance in the AUV's data. The authors also thank the personnel of "Arsenal do Alfeite" and of CINAV for allowing conditions for the usage of the calibration tank. This work was funded under WiMUST project (contract 645141) of the European Union H2020 program.

REFERÊNCIAS

- ¹ C. H. Sherman and J. L. Butler, "Transducers and Arrays for Underwater Sound", *Springer, The Underwater Acoustic series*, (2007).
- ² J. C. Shipps and B. M. Abraham, "The Use of Vector Sensors for Underwater Port and Waterway Security", *Proceedings of Sensors for Industry conference, New Orleans, Louisiana, USA*, 41-44 (2004).
- ³ A. Nehorai and E. Paldi, "Vector-Sensor Array Processing for electromagnetic source localization", *IEEE Trans. Signal Processing* **42-2**, 376-398 (1994).
- ⁴ A. Nehorai and E. Paldi, "Acoustic Vector-Sensor Array Processing", *IEEE Trans. Signal Processing*, **42-9**, 2481-2491 (1994).
- ⁵ M. Hawkes and A. Nehorai, "Acoustic Vector-Sensor beamforming and Capon direction estimation, *IEEE Trans. Signal Processing* **46-9**, 2291-2304 (1998)
- ⁶ B. A. Cray and A. H. Nuttall, "Directivity factors for linear arrays of velocity sensors, *J. Acoust. Soc. Am.* **110-1**, 324-331 (2001).
- ⁷ C. Wan, A. Kong and C. Liu, "A comparative study of DOA estimation using vector/gradient sensors", *Proceedings of Oceans'06, Asia, Pacific*, 1-4 (2007).

-
- ⁸ K. M. Krishna and G. V. Anand, "Narrowband detection of acoustic source in shallow ocean using vector sensor array", *Proceedings of Oceans 2009 MTS/IEEE, USA*, 1-8 (2009).
- ⁹ V. N. Hari, G. V. Anand, A. B. Premkumar and A. S. Madhukumar, "Underwater signal detection in partially known ocean using short acoustic vector sensor array", *Proceedings of Oceans 11 IEEE/OES Santander Conference, Spain*, 1-9 (2011).
- ¹⁰ P. Felisberto, P. Santos and S. M. Jesus, "Tracking source azimuth using a single vector sensor", *Proceedings of 4th Int. Conference on Sensor Technologies and Applications, Italy*, 416-421 (2010).
- ¹¹ A. Abdi, H. Guo and P. Sutthiwan, "A new vector sensor receiver for underwater acoustic communication", *Proceedings MTS/IEEE Oceans, Vancouver, BC, Canada*, 1-10 (2007).
- ¹² A. Song, M. Badiy, P. Hursky and A. Abdi, "Time reversal receivers for underwater acoustic communication using vector sensors", *IEEE, Quebec, Canada*, 1-10 (2008).
- ¹³ H. Peng and F. Li, "Geoacoustic Inversion based on a Vector Hydrophone Array", *Chin. Phys. Lett.*, **24-7**, 1977-1980 (2007).
- ¹⁴ P. Santos, O. C. Rodríguez, P. Felisberto and S. M. Jesus, "Seabed geoacoustic Characterization with a Vector Sensor Array", *J. Acoust. Soc. Am.* **128-5**, 2652-2663 (2010).
- ¹⁵ P. Felisberto, P. Santos, D. Maslov and S. M. Jesus, "Combining pressure and particle velocity sensors for seismic processing", *Proc. MTS/IEEE/OES Oceans'16, USA* (2016).
- ¹⁶ "An overview of marine seismic operations", *OGP - International Association of Oil & Gas Producers and IAGC - International Association of Geophysical Contractors*, Report **448** (2011).
- ¹⁷ A. Mantouka, P. Felisberto, P. Santos, F. Zabel, M. Saleiro, S. M. Jesus and L. Sebastião, "Development and testing of a Dual Accelerometer Vector Sensor for AUV acoustic surveys", *Sensors*, **17-1328**, 1-12 (2017).
- ¹⁸ P. C. Abreu, J. Botelho, P. Góis, A. Pascoal, J. Ribeiro, M. Ribeiro, M. Rufino, L. Sebastião and H. Silva, "The MEDUSA class of autonomous marine vehicles and their role in EU projects", *Proc. of Oceans'16 Shangai IEEE Conference, China* (2016).
- ¹⁹ P. Felisberto, O. C. Rodríguez, P. Santos, E. Ey and S. M. Jesus, "Experimental results of Underwater Cooperative Source Localization using a single Vector Sensor", *Sensors* **13-7**, 8856-8878 (2013).
-